FUMI, F. G. (1952*c*). *Nuovo Cim.* **9**, 739–755.
FUMI, F. G. (1953). *Nuovo Cim.* **10**, 865–882.
GHATE, P. B. (1964). *J. Appl. Phys.* **35**, 337–339.
GHATE, P. B. (1965). *Indian J. Phys.* **39**, 257–264.
GRAHAM, R. A. (1972). *J. Acoust. Soc. Amer.* **51**, 1576–1581.
HEARMON, R. F. S. (1953). *Acta Cryst.* **6**, 331–341.
KRISHNAMURTY, T. S. G. (1963). *Acta Cryst.* **16**, 839–840.
KRISHNAMURTY, T. S. G. & GOPALAKRISHNAMURTY, P. (1968). *Acta Cryst.* A**24**, 563–564.
LEAN, E. G. & TSENG, C. C. (1970). *J. Appl. Phys.* **41**, 3912–3917.
LJAMOV, V. E. (1972). *J. Acoust. Soc. Amer.* **52**, 199–202.
LJAMOV, V. E., HSU, T. H. & WHITE, R. M. (1972). *J. Appl. Phys.* **43**, 800–806.
MCMAHON, D. H. (1968). *J. Acoust. Soc. Amer.* **44**, 1007–1013.
MATHUS, S. S. & GUPTA, P. N. (1970). *Acoustica*, **23**, 160–164.
PETERS, R. D. & ARNOLD, R. T. (1971). *J. Appl. Phys.* **42**, 980–983.
RICHARDSON, B. A., THOMPSON, R. B. & WILKINSON, C. D. W. (1968). *J. Acoust. Soc. Amer.* **44**, 1608–1615.

Acta Cryst. (1974). A**30**, 13

The Crystal-Structural Transformation NaCl-type → CsCl-type: Analysis by Martensite Theory

BY W. L. FRASER AND S. W. KENNEDY

Department of Physical and Inorganic Chemistry, University of Adelaide, Adelaide, S.A. 5001, *Australia*

(*Received* 24 *July* 1973; *accepted* 28 *August* 1973)

Orientation relations, interface (habit plane) orientations, and shape changes have been computed by martensite theory for the crystal-structural transformation NaCl-type (f.c.c.) → CsCl-type (primitive cubic), especially in alkali halides. The lattice correspondence used involves contraction along the three-fold axis of a primitive rhombohedron of f.c.c. For the matrix analysis a computer program was written in FORTRAN. Mathematical solutions were obtained using two lattice-invariant shears based on slip and one based on transformation twinning. There are three types of solution. Within each of the three types multiplicity due to symmetry leads to 24 variants. Possible habit planes are near to $\{\bar{1}11\}_I$, $\{210\}_I$ and $\{310\}_I$. Shape changes are large. Predictions agree with observations within experimental error. As the principles applied need not exclude some changes of stoichiometry, they may be relevant to topotaxy.

1. Introduction

Transformation between the NaCl and CsCl structures provides a test of the magnitude of structure change that can proceed martensitically in ionic crystals. Elucidation of the mechanism may also be relevant to topotactic reactions between compounds structurally related to these. Transformations between these structures in the alkali halides at normal or high pressure are also of some technological interest. The transformation of the NaCl to the CsCl structure involves a change of first coordination, from 6 to 8, associated in all known examples with a large volume change, $\Delta V/V_{CsCl} = 17\%$. Martensite theory, which has mainly been applied to alloys, should facilitate description of many structural changes in macroscopic non-metallic crystals, and have special value when there is a large change of lattice. Recent experiments by Fraser & Kennedy (1972) and Livshitz, Ryabinin, Larionov & Zverev (1969) indicate that, under some circumstances, the transformation NaCl-type ⇄ CsCl-type is indeed martensitic. Such experiments provide some data against which to compare predictions, which themselves can serve as a guide to the interpretation of observations.

The present work uses martensite theory to predict orientation relations, interface orientations and shape changes in martensitic transformation from the NaCl structure to the CsCl structure. The analysis is similar for a series of salts because the ratios of the lattice parameters are similar. Results are presented for CsCl, NH_4Cl, NH_4Br and NH_4I, and also for a sufficient range of ratio of lattice parameters to include KCl and other alkali halides which transform under pressure. All these compounds have the NaCl structure in phase I and the CsCl structure in phase II.

2. Theory

2.1 *General principles*

An introduction to martensite theory is given by Kelly & Groves (1970) and by Owen & Shoen (1971). Wayman (1964) and Christian (1965) provide more detailed accounts. Numerous reviews include a recent one by Bowles & Wayman (1972). Original statements of the theory are by Bowles & Mackenzie (1954), and Wechsler, Lieberman & Read (1953). These treatments were applied to metallic alloys. As a different lattice deformation has been used for this transformation, the mathematical analysis has been correspondingly mod-

ified. Fundamentals are stated here to provide a convenient basis for discussion of ionic compounds.

Martensite theory can be applied if a suitable cell can be converted into the new arrangement by a deformation. The cell, if primitive, may correspond to a coordination polyhedron as in the present example, in which the lattice deformation provides the required new arrangement of ions directly. Corresponding displacements of ions could occur across the boundary between parent and product without diffusive interchange if the two lattices remain in register to within atomic dimensions over macroscopic distances. In general there is no plane of the product which so closely corresponds to any plane of the parent, but the accumulating misfit on some plane of approximate fit can be corrected periodically either by change to another symmetry-equivalent deformation, or by an additional displacement in one direction. The former leads to transformation twinning (the twin plane being a mirror plane of the parent), the latter leads to propagation of a slip texture in the product. In either case, the effect averaged over many unit cells is a shear additional to the deformation which would suffice to transform the lattices and known as the 'lattice-invariant shear'. With this two-dimensional fit, a large volume change can be achieved by a component of expansion normal to this plane of average fit – the 'habit plane'. The combination of deformations necessarily produces a displacement resulting in a shape change at the surface of the specimen. It may be significant for chemical reactions that these concepts do not exclude some change of stoichiometry.

The data required are the lattice parameters, the symmetry relation involved in the lattice deformation (this underlies the transformation twinning), and the slip modes of the product. It is implied not that the product slips because of mechanical stress, (though it may do so subsequently), but that the slip modes correspond to relatively low-energy dislocations which may also operate in lattice-invariant displacements as the new structure is formed.

2.2 *The lattice correspondence and deformation*

A differential dilation (pure strain) which interconverts the f.c.c. NaCl and primitive cubic CsCl structures by relative contraction along a threefold axis (Fig. 1) was pointed out by Shoji (1931), who also suggested that this formal relation would not represent the probable orientation relation. Zintl & Brauer (1935) illustrated the structural relation. This was also Buerger's (1951, 1961) example of a dilatational transformation, in which the higher energy barriers involved in diffusional rearrangement were avoided. In this pure strain there is a 40% contraction along a $\langle 111 \rangle$ direction of the f.c.c. lattice accompanied by an expansion of 19% in all directions normal to this, in typical substances. That is, the principal distortions are $\eta_3(\|[111]) = 0{\cdot}6$ and $\eta_1 = \eta_2 = 1{\cdot}19$. The lattice correspondence is here defined by:

$$\begin{pmatrix} \frac{1}{2} & \frac{1}{2} & 0 \\ 0 & \frac{1}{2} & \frac{1}{2} \\ \frac{1}{2} & 0 & \frac{1}{2} \end{pmatrix} \bar{\mathbf{x}}_{\mathrm{II}} = \bar{\mathbf{x}}_{\mathrm{I}}$$

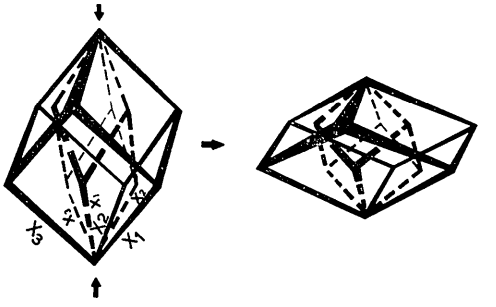

Fig. 1. The lattice deformation. A contraction of approximately 40% in a $\langle 111 \rangle_{\mathrm{I}}$ direction accompanied by a perpendicular expansion of approximately 19% converts the primitive rhombohedron of the f.c.c. cell into a primitive cube. In so doing, the face-centred cell becomes rhombohedral with interedge angles of 70·53 and 109·47° ($\langle 100 \rangle_{\mathrm{I}} \rightarrow \langle 111 \rangle_{\mathrm{II}}$). The choice of axes is also shown.

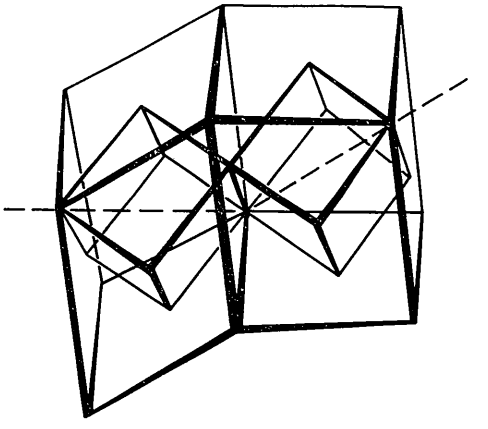

Fig. 2. $\{100\}\langle 110 \rangle_{\mathrm{I}}$ transformation twins. Contraction axes in neighbouring volumes of NaCl structure are related by reflexion in 100_{I} ($\rightarrow \{110\}_{\mathrm{II}}$) planes. The ions on each side undergo mirror-related displacements such that the lattice is continuous across the 'twin' boundary, *i.e.* transformation 'twinning' leads to a single-crystal product. The dashed lines denote the $\langle 111 \rangle$ contraction axes.

Table 1. *Equilibrium temperatures, lattice parameters and deformations*

Substance	T(°C)	Lattice parameters a_{I}(Å)	a_{II}(Å)	$a_{\mathrm{I}}/a_{\mathrm{II}}$	η_1	η_3	φ	φ^1
CsCl	469	$7{\cdot}07_4$	$4{\cdot}22_4$	$1{\cdot}67_5$	1·194	0·597	50°53′	67°53′
NH_4Cl	183·1	6·61	3·92	$1{\cdot}68_6$	1·186	0·593	51°39′	68°25′
NH_4Br	137·2	6·86	4·09	$1{\cdot}67_7$	1·192	0·596	51°4′	68°0′
NH_4I	−16	7·25	$4{\cdot}33_5$	$1{\cdot}67_2$	1·196	0·598	50°42′	67°45′

Table 2. *Solutions for the lattice-invariant (L.I.) shear* $(10\bar{1})\,[010]_{II}/(1\bar{1}0)\,[110]_{I}$

L.I. shear angle in product (parent) (°)	Rotation axis	Rotation (°)	Habit plane indices	Direction of shape strain	Magnitude of shape strain
(*a*) CsCl, $a_I/a_{II}=1{\cdot}675$					
(1)	(*a*)				
$-14{\cdot}9_6$ ($-20{\cdot}7_0$)	$\begin{bmatrix} -0{\cdot}340 \\ 0{\cdot}236 \\ 0{\cdot}910 \end{bmatrix}_I$	$40{\cdot}2_5$	$(-0{\cdot}202$ $-0{\cdot}978$ $0{\cdot}057)_I$	$\begin{bmatrix} 0{\cdot}751 \\ 0{\cdot}031 \\ 0{\cdot}590 \end{bmatrix}_I$	0·956
	(*b*)				
	$\begin{bmatrix} 0{\cdot}939 \\ -0{\cdot}272 \\ -0{\cdot}211 \end{bmatrix}_I$	$19{\cdot}8_0$	$(0{\cdot}663$ $-0{\cdot}418$ $0{\cdot}621)_I$	$\begin{bmatrix} -0{\cdot}503 \\ -0{\cdot}780 \\ -0{\cdot}227 \end{bmatrix}_I$	0·956
(2)	(*a*)				
$14{\cdot}9_6$ ($20{\cdot}7_0$)	$\begin{bmatrix} -0{\cdot}236 \\ 0{\cdot}340 \\ -0{\cdot}910 \end{bmatrix}$	$40{\cdot}2_5$	$(-0{\cdot}978$ $-0{\cdot}202$ $0{\cdot}057)_I$	$\begin{bmatrix} 0{\cdot}031 \\ 0{\cdot}751 \\ 0{\cdot}590 \end{bmatrix}_I$	0·956
	(*b*)				
	$\begin{bmatrix} 0{\cdot}272 \\ -0{\cdot}939 \\ 0{\cdot}211 \end{bmatrix}_I$	$19{\cdot}8_0$	$(-0{\cdot}418$ $0{\cdot}663$ $0{\cdot}621)_I$	$\begin{bmatrix} -0{\cdot}780 \\ -0{\cdot}503 \\ -0{\cdot}227 \end{bmatrix}_I$	0·956
(*b*) NH_4Cl, $a_I/a_{II}=1{\cdot}686$					
(1)	(*a*)				
$-14{\cdot}2_3$ ($-19{\cdot}7_3$)	$\begin{bmatrix} -0{\cdot}354 \\ 0{\cdot}236 \\ 0{\cdot}905 \end{bmatrix}_I$	$38{\cdot}8_8$	$(-0{\cdot}214$ $-0{\cdot}976$ $0{\cdot}046)_I$	$\begin{bmatrix} 0{\cdot}720 \\ 0{\cdot}040 \\ 0{\cdot}581 \end{bmatrix}_I$	0·927
	(*b*)				
	$\begin{bmatrix} 0{\cdot}939 \\ -0{\cdot}267 \\ -0{\cdot}219 \end{bmatrix}_I$	$19{\cdot}6_3$	$(0{\cdot}663$ $-0{\cdot}400$ $0{\cdot}633)_I$	$\begin{bmatrix} -0{\cdot}487 \\ -0{\cdot}754 \\ -0{\cdot}228 \end{bmatrix}_I$	0·927
(2)	(*a*)				
$14{\cdot}2_3$ ($19{\cdot}7_3$)	$\begin{bmatrix} -0{\cdot}236 \\ 0{\cdot}354 \\ -0{\cdot}905 \end{bmatrix}_I$	$38{\cdot}8_8$	$(-0{\cdot}976$ $-0{\cdot}214$ $0{\cdot}046)_I$	$\begin{bmatrix} 0{\cdot}040 \\ 0{\cdot}720 \\ 0{\cdot}581 \end{bmatrix}_I$	0·927
	(*b*)				
	$\begin{bmatrix} 0{\cdot}267 \\ -0{\cdot}939 \\ -0{\cdot}219 \end{bmatrix}_I$	$19{\cdot}6_3$	$(-0{\cdot}400$ $0{\cdot}663$ $0{\cdot}633)_I$	$\begin{bmatrix} -0{\cdot}754 \\ -0{\cdot}487 \\ -0{\cdot}228 \end{bmatrix}_I$	0·927
(*c*) NH_4Br, $a_I/a_{II}=1{\cdot}677$					
(1)	(*a*)				
$-14{\cdot}8_0$ ($-20{\cdot}4_8$)	$\begin{bmatrix} -0{\cdot}344 \\ 0{\cdot}236 \\ 0{\cdot}909 \end{bmatrix}_I$	$39{\cdot}9_4$	$(-0{\cdot}204$ $-0{\cdot}977$ $0{\cdot}054)_I$	$\begin{bmatrix} 0{\cdot}744 \\ 0{\cdot}033 \\ 0{\cdot}588 \end{bmatrix}_I$	0·949
	(*b*)				
	$\begin{bmatrix} 0{\cdot}939 \\ -0{\cdot}271 \\ -0{\cdot}213 \end{bmatrix}_I$	$19{\cdot}7_6$	$(0{\cdot}663$ $-0{\cdot}414$ $0{\cdot}623)_I$	$\begin{bmatrix} -0{\cdot}499 \\ -0{\cdot}774 \\ -0{\cdot}227 \end{bmatrix}_I$	0·949
(2)	(*a*)				
$14{\cdot}8_0$ ($20{\cdot}4_8$)	$\begin{bmatrix} -0{\cdot}236 \\ 0{\cdot}344 \\ -0{\cdot}909 \end{bmatrix}_I$	$39{\cdot}9_4$	$(-0{\cdot}977$ $-0{\cdot}204$ $0{\cdot}054)_I$	$\begin{bmatrix} 0{\cdot}033 \\ 0{\cdot}744 \\ 0{\cdot}588 \end{bmatrix}_I$	0·949
	(*b*)				
	$\begin{bmatrix} 0{\cdot}271 \\ -0{\cdot}939 \\ 0{\cdot}213 \end{bmatrix}_I$	$19{\cdot}7_6$	$(-0{\cdot}414$ $0{\cdot}663$ $0{\cdot}623)_I$	$\begin{bmatrix} -0{\cdot}774 \\ -0{\cdot}499 \\ -0{\cdot}227 \end{bmatrix}_I$	0·949

(*d*) NH_4I, $a_I/a_{II}=1{\cdot}672$. Solutions identical to those for CsCl within the precision of these Tables.

Table 3. *Solutions for lattice-invariant (L.I.) shear* (110) $[001]_{II}/(100)\ [011]_{I}$

L.I. shear angle in product (parent) (°)	Rotation axis	Rotation (°)	Habit plane indices	Direction of shape strain	Magnitude of shape strain
(*a*) CsCl, $a_I/a_{II}=1{\cdot}675$					
(1)	(*a*)				
$-10{\cdot}4_1$	$\begin{bmatrix}0{\cdot}252\\0{\cdot}888\\-0{\cdot}385\end{bmatrix}_I$	$32{\cdot}1_9$	$\begin{pmatrix}-0{\cdot}472\\-0{\cdot}087\\0{\cdot}877\end{pmatrix}_I$	$\begin{bmatrix}0{\cdot}271\\-0{\cdot}393\\-0{\cdot}062\end{bmatrix}_I$	0·481
$(27{\cdot}6_3)$	(*b*)				
	$\begin{bmatrix}-0{\cdot}252\\0{\cdot}385\\-0{\cdot}888\end{bmatrix}_I$	$32{\cdot}1_9$	$\begin{pmatrix}0{\cdot}472\\-0{\cdot}877\\0{\cdot}087\end{pmatrix}_I$	$\begin{bmatrix}-0{\cdot}271\\0{\cdot}062\\0{\cdot}393\end{bmatrix}_I$	0·481
(2)	(*a*)				
$-27{\cdot}6_3$	$\begin{bmatrix}0{\cdot}668\\0{\cdot}073\\-0{\cdot}741\end{bmatrix}_I$	$17{\cdot}0_0$	$\begin{pmatrix}0{\cdot}472\\-0{\cdot}087\\0{\cdot}877\end{pmatrix}_I$	$\begin{bmatrix}-0{\cdot}271\\-0{\cdot}393\\-0{\cdot}062\end{bmatrix}_I$	0·481
$(10{\cdot}4_1)$	(*b*)				
	$\begin{bmatrix}-0{\cdot}668\\0{\cdot}741\\-0{\cdot}073\end{bmatrix}_I$	$17{\cdot}0_0$	$\begin{pmatrix}-0{\cdot}472\\-0{\cdot}877\\0{\cdot}087\end{pmatrix}_I$	$\begin{bmatrix}0{\cdot}271\\0{\cdot}062\\0{\cdot}393\end{bmatrix}_I$	0·481
(*b*) NH_4Cl, $a_I/a_{II}=1{\cdot}686$					
(1)	(*a*)				
$-10{\cdot}0_2$	$\begin{bmatrix}0{\cdot}249\\0{\cdot}887\\-0{\cdot}389\end{bmatrix}_I$	$32{\cdot}5_4$	$\begin{pmatrix}-0{\cdot}478\\-0{\cdot}069\\0{\cdot}876\end{pmatrix}_I$	$\begin{bmatrix}0{\cdot}274\\-0{\cdot}391\\-0{\cdot}071\end{bmatrix}_I$	0·483
$(27{\cdot}9_4)$	(*b*)				
	$\begin{bmatrix}-0{\cdot}249\\0{\cdot}389\\-0{\cdot}887\end{bmatrix}_I$	$32{\cdot}5_4$	$\begin{pmatrix}-0{\cdot}478\\-0{\cdot}876\\0{\cdot}069\end{pmatrix}_I$	$\begin{bmatrix}-0{\cdot}274\\0{\cdot}071\\0{\cdot}391\end{bmatrix}_I$	0·483
(2)	(*a*)				
$-27{\cdot}9_4$	$\begin{bmatrix}0{\cdot}676\\0{\cdot}058\\-0{\cdot}734\end{bmatrix}_I$	$16{\cdot}7_8$	$\begin{pmatrix}0{\cdot}478\\-0{\cdot}069\\0{\cdot}876\end{pmatrix}_I$	$\begin{bmatrix}-0{\cdot}274\\-0{\cdot}391\\-0{\cdot}071\end{bmatrix}_I$	0·483
$(10{\cdot}0_2)$	(*b*)				
	$\begin{bmatrix}-0{\cdot}676\\0{\cdot}734\\-0{\cdot}058\end{bmatrix}_I$	$16{\cdot}7_8$	$\begin{pmatrix}-0{\cdot}478\\-0{\cdot}876\\0{\cdot}069\end{pmatrix}_I$	$\begin{bmatrix}0{\cdot}274\\0{\cdot}071\\0{\cdot}391\end{bmatrix}_I$	0·483
(*c*) NH_4Br, $a_I/a_{II}=1{\cdot}677$					
(1)	(*a*)				
$-10{\cdot}3_2$	$\begin{bmatrix}0{\cdot}251\\0{\cdot}888\\-0{\cdot}386\end{bmatrix}_I$	$32{\cdot}2_7$	$\begin{pmatrix}-0{\cdot}474\\-0{\cdot}083\\0{\cdot}877\end{pmatrix}_I$	$\begin{bmatrix}0{\cdot}272\\-0{\cdot}392\\-0{\cdot}064\end{bmatrix}_I$	0·481
$(27{\cdot}7_0)$	(*b*)				
	$\begin{bmatrix}-0{\cdot}251\\0{\cdot}386\\-0{\cdot}888\end{bmatrix}_I$	$32{\cdot}2_7$	$\begin{pmatrix}0{\cdot}474\\-0{\cdot}877\\0{\cdot}083\end{pmatrix}_I$	$\begin{bmatrix}-0{\cdot}272\\0{\cdot}064\\0{\cdot}392\end{bmatrix}_I$	0·481
(2)	(*a*)				
$-27{\cdot}7_0$	$\begin{bmatrix}0{\cdot}670\\0{\cdot}070\\-0{\cdot}739\end{bmatrix}_I$	$16{\cdot}9_5$	$\begin{pmatrix}0{\cdot}474\\-0{\cdot}083\\0{\cdot}877\end{pmatrix}_I$	$\begin{bmatrix}-0{\cdot}272\\-0{\cdot}392\\-0{\cdot}064\end{bmatrix}_I$	0·481
$(10{\cdot}3_2)$	(*b*)				
	$\begin{bmatrix}-0{\cdot}670\\0{\cdot}739\\-0{\cdot}070\end{bmatrix}_I$	$16{\cdot}9_5$	$\begin{pmatrix}-0{\cdot}474\\-0{\cdot}877\\0{\cdot}083\end{pmatrix}_I$	$\begin{bmatrix}0{\cdot}272\\0{\cdot}064\\0{\cdot}392\end{bmatrix}_I$	0·481

(*d*) NH_4I, $a_I/a_{II}=1{\cdot}672$. Solutions identical to those for CsCl within the precision of these Tables.

where $\bar{\mathbf{x}}_I$ and $\bar{\mathbf{x}}_{II}$ are vectors in the f.c.c. and primitive cells respectively and Fig. 1 shows the choice of axes. The pure lattice strain alone corresponds to the orientation relation $[111]_I \| [111]_{II}$, $(\bar{1}10_I) \| (\bar{1}01)_{II}$.

The condition that parent and product remain in register implies that lengths and directions of vectors remain unaltered in the plane of contact: it is an invariant plane when averaged over many unit cells. Vectors which are unaltered in length (though their positions are altered) by the pure lattice strain alone lie on the surface of a cone (Fig. 3). The semi-apex angles of initial (φ) and final (φ') cones are given by: $\tan\varphi = [(1-\eta_3^2)/(\eta_1^2-1)]^{1/2}$ and $\tan\varphi' = (\eta_1/\eta_3)\tan\varphi$. In moving from the initial to the final cone, any two vectors alter their included angle. The plane defined by them is therefore extended: no plane remains unaltered. The lattice-invariant shear accommodates the misfit for particular planes.

2.3 *The lattice-invariant shear and total deformation*

The mathematical problem is to determine the amount of lattice-invariant shear (described by matrix $\mathbf{P}_1$) necessary to maintain an undeformed plane during the transformation, when the transformation of the lattice is achieved by the pure strain, described by matrix **B**. Since the undeformed plane is to remain common to the phases (invariant), the product must in general grow in an orientation different from that given by **B**: the difference is a rotation given by matrix **R**. The total shape strain **P**, which is an 'invariant-plane strain', is given by $\mathbf{P} = \mathbf{RP}_1\mathbf{B}$. It is convenient, however, to refer the lattice-invariant shear to the untransformed parent lattice. The shear is then represented by matrix $\mathbf{P}_2$, where $\mathbf{P} = \mathbf{RBP}_2$. The lattice transformation produces the elements of $\mathbf{P}_1$ from $\mathbf{P}_2$. Generally, there are two solutions for the amount of lattice-invariant shear: each of these corresponds to two

Table 4. 2% *change of lattice parameter, lattice-invariant (L.I.) shear* $= (\bar{1}01)\,[010]_{II}/(1\bar{1}0)\,[110]_I$: NH_4Br

L.I. shear angle in product (parent) (°)	Rotation axis	Rotation (°)	Habit plane indices	Direction of shape strain	Magnitude of shape strain
(*a*) $a_I/a_{II} = 1{\cdot}645$ (+2% in a_{II} or −2% in a_I)					
(1)	(*a*)				
$-16{\cdot}9_9$	$\begin{bmatrix} -0{\cdot}303 \\ 0{\cdot}236 \\ 0{\cdot}923 \end{bmatrix}_I$	$44{\cdot}0_2$	$(-0{\cdot}170$ $-0{\cdot}982$ $0{\cdot}083)_I$	$\begin{bmatrix} 0{\cdot}839 \\ 0{\cdot}010 \\ 0{\cdot}613 \end{bmatrix}_I$	1·04
$(-23{\cdot}3_7)$	(*b*)				
	$\begin{bmatrix} 0{\cdot}939 \\ -0{\cdot}286 \\ -0{\cdot}191 \end{bmatrix}_I$	$20{\cdot}1_8$	$(0{\cdot}665$ $-0{\cdot}464$ $0{\cdot}585)$	$\begin{bmatrix} -0{\cdot}551 \\ -0{\cdot}853 \\ -0{\cdot}224 \end{bmatrix}_I$	1·04
(2)	(*a*)				
$16{\cdot}9_9$	$\begin{bmatrix} -0{\cdot}236 \\ 0{\cdot}303 \\ -0{\cdot}923 \end{bmatrix}_I$	$44{\cdot}0_2$	$(-0{\cdot}982$ $-0{\cdot}170$ $0{\cdot}083)_I$	$\begin{bmatrix} 0{\cdot}010 \\ 0{\cdot}839 \\ 0{\cdot}613 \end{bmatrix}_I$	1·04
$(23{\cdot}3_7)$	(*b*)				
	$\begin{bmatrix} 0{\cdot}286 \\ -0{\cdot}939 \\ 0{\cdot}191 \end{bmatrix}_I$	$20{\cdot}1_8$	$(-0{\cdot}464$ $0{\cdot}665$ $0{\cdot}585)_I$	$\begin{bmatrix} -0{\cdot}853 \\ -0{\cdot}551 \\ -0{\cdot}224 \end{bmatrix}_I$	1·04
(*b*) $a_I/a_{II} = 1{\cdot}711$ (−2% in a_{II} or +2% in a_I)					
(1)	(*a*)				
$-12{\cdot}7_5$	$\begin{bmatrix} -0{\cdot}384 \\ 0{\cdot}236 \\ 0{\cdot}893 \end{bmatrix}_I$	$36{\cdot}1_1$	$(-0{\cdot}238$ $-0{\cdot}971$ $0{\cdot}022)_I$	$\begin{bmatrix} 0{\cdot}662 \\ 0{\cdot}058 \\ 0{\cdot}562 \end{bmatrix}_I$	0·870
$(-17{\cdot}7_4)$	(*b*)				
	$\begin{bmatrix} 0{\cdot}937 \\ -0{\cdot}258 \\ -0{\cdot}236 \end{bmatrix}_I$	$19{\cdot}2_1$	$(0{\cdot}661$ $-0{\cdot}358$ $0{\cdot}659)_I$	$\begin{bmatrix} -0{\cdot}456 \\ -0{\cdot}704 \\ -0{\cdot}230 \end{bmatrix}_I$	0·870
(2)	(*a*)				
$12{\cdot}7_5$	$\begin{bmatrix} -0{\cdot}236 \\ 0{\cdot}384 \\ -0{\cdot}893 \end{bmatrix}_I$	$36{\cdot}1_1$	$(-0{\cdot}971$ $-0{\cdot}238$ $0{\cdot}022)_I$	$\begin{bmatrix} 0{\cdot}058 \\ 0{\cdot}662 \\ 0{\cdot}562 \end{bmatrix}_I$	0·870
$(17{\cdot}7_4)$	(*b*)				
	$\begin{bmatrix} 0{\cdot}258 \\ -0{\cdot}937 \\ 0{\cdot}236 \end{bmatrix}_I$	$19{\cdot}2_1$	$(-0{\cdot}358$ $0{\cdot}661$ $0{\cdot}659)_I$	$\begin{bmatrix} -0{\cdot}704 \\ -0{\cdot}456 \\ -0{\cdot}230 \end{bmatrix}_I$	0·870

possible invariant planes. For any one proposed lattice-invariant shear system there are therefore four solutions, each predicting an interface, orientation relation and shape change. This number will be increased by the existence of symmetry-equivalent choices of shear systems.

The choices of lattice-invariant (L.I.) shears for the calculations were based on the possible transformation twinning, and on the known modes of slip (translation gliding) of the product structure type.

2.3.1 *Slip modes*

The reported slip modes for the CsCl structure (Rachinger & Cottrell, 1956) are the six $\{110\}\langle001\rangle_{II}$. Three of these (set *A*) contain the principal strain axis $[111]_{II}$, and three (set *B*) do not. The two sets are:

A, $(1\bar{1}0)\,[001]_{II}$, $(0\bar{1}1)\,[100]_{II}$, $(\bar{1}01)\,[010]_{II}$;

B, $(110)\,[001]_{II}$, $(011)\,[100]_{II}$, $(101)\,[010]_{II}$.

2.3.2 *Transformation twinning*

Transformation twinning results from contraction along different $\langle111\rangle_I$ principal strain axes in adjacent regions. Pairs of $\langle111\rangle_I$ in cubic cells are related by reflexion in $\{100\}$ or $\{110\}$. In general, twin planes of the product are derived from such mirror planes of the parent. There are, therefore, two possible types.

(*a*) A type derived from $\{110\}_I$. The twinning shear systems are $(121)\,[1\bar{1}1]_{II}$, $(211)\,[\bar{1}11]_{II}$, $(112)\,[11\bar{1}]_{II}$. The L.I. shear plane is required to cut the cone of unextended vectors. Stereograms show that these shear planes do not do so. This type of lattice-invariant shear is therefore not capable of correcting the interfacial misregistry.

(*b*) A type derived from $\{100\}_I$. Twin shears $(110)\,[001]_{II}$, $(011)\,[100]_{II}$, $(101)\,[010]_{II}$ are derived from $(100)\,[011]_I$, $(010)\,[101]_I$, $(001)\,[110]_I$. Because of the cubic symmetry of the product, this is a special case, resulting in a novel example of transformation twinning

Table 5. 2% *change of lattice parameter, lattice-invariant (L.I.) shear* = $(110)\,[001]_{II}/(100)\,[011]_I$: NH_4Br

L.I. shear angle in product (parent) (°)	Rotation axis	Rotation (°)	Habit plane indices	Direction of shape strain	Magnitude of shape strain
(*a*) $a_I/a_{II}=1{\cdot}645$ (+2% in a_{II} or −2% in a_I)					
(1)	(*a*)				
$-11{\cdot}4_I$	$\begin{bmatrix}0{\cdot}257\\0{\cdot}890\\-0{\cdot}376\end{bmatrix}_I$	$31{\cdot}2_4$	$(-0{\cdot}455\ -0{\cdot}132\ 0{\cdot}881)_I$	$\begin{bmatrix}0{\cdot}264\\-0{\cdot}395\\-0{\cdot}038\end{bmatrix}_I$	0·477
$(26{\cdot}8_I)$	(*b*)				
	$\begin{bmatrix}-0{\cdot}257\\0{\cdot}376\\-0{\cdot}890\end{bmatrix}_I$	$31{\cdot}2_4$	$(0{\cdot}455\ -0{\cdot}881\ 0{\cdot}132)_I$	$\begin{bmatrix}-0{\cdot}264\\0{\cdot}038\\0{\cdot}395\end{bmatrix}_I$	0·477
(2)	(*a*)				
$-26{\cdot}8_I$	$\begin{bmatrix}0{\cdot}643\\0{\cdot}114\\-0{\cdot}757\end{bmatrix}$	$17{\cdot}5_2$	$(0{\cdot}455\ -0{\cdot}132\ 0{\cdot}881)_I$	$\begin{bmatrix}-0{\cdot}264\\-0{\cdot}395\\-0{\cdot}038\end{bmatrix}$	0·477
$(11{\cdot}4_I)$	(*b*)				
	$\begin{bmatrix}-0{\cdot}643\\0{\cdot}757\\-0{\cdot}114\end{bmatrix}_I$	$17{\cdot}5_2$	$(-0{\cdot}455\ -0{\cdot}881\ 0{\cdot}132)_I$	$\begin{bmatrix}0{\cdot}264\\0{\cdot}038\\0{\cdot}395\end{bmatrix}_I$	0·477
(*b*) $a_I/a_{II}=1{\cdot}711$ (−2% in a_{II} or +2% in a_I)					
(1)	(*a*)				
$-9{\cdot}20_5$	$\begin{bmatrix}0{\cdot}243\\0{\cdot}884\\-0{\cdot}399\end{bmatrix}_I$	$33{\cdot}2_4$	$(-0{\cdot}490\ -0{\cdot}032\ 0{\cdot}871)_I$	$\begin{bmatrix}0{\cdot}278\\-0{\cdot}388\\-0{\cdot}088\end{bmatrix}_I$	0·486
$(28{\cdot}5_9)$	(*b*)				
	$\begin{bmatrix}-0{\cdot}243\\0{\cdot}399\\-0{\cdot}884\end{bmatrix}_I$	$33{\cdot}2_4$	$(0{\cdot}490\ -0{\cdot}871\ 0{\cdot}032)_I$	$\begin{bmatrix}-0{\cdot}278\\0{\cdot}088\\0{\cdot}388\end{bmatrix}_I$	0·486
(2)	(*a*)				
$-28{\cdot}5_9$	$\begin{bmatrix}0{\cdot}694\\0{\cdot}026\\-0{\cdot}720\end{bmatrix}_I$	$16{\cdot}2_7$	$(0{\cdot}490\ -0{\cdot}032\ 0{\cdot}871)_I$	$\begin{bmatrix}-0{\cdot}278\\-0{\cdot}388\\-0{\cdot}088\end{bmatrix}_I$	0·486
$(9{\cdot}20_5)$	(*b*)				
	$\begin{bmatrix}-0{\cdot}694\\0{\cdot}720\\-0{\cdot}026\end{bmatrix}_I$	$16{\cdot}2_7$	$(-0{\cdot}490\ -0{\cdot}871\ 0{\cdot}032)_I$	$\begin{bmatrix}0{\cdot}278\\0{\cdot}088\\0{\cdot}388\end{bmatrix}_I$	0·486

which would be noticeable only as surface displacements. The 'twin' plane is a mirror plane also of phase II, the lattice of which is therefore not twinned (Fig. 2). Nevertheless, the displacements involved are twin-related: if regions of product produced by each of two twin-related displacements are present, the net effect is an average shear as required. The solutions for these 'twinning' modes are the same as for the slip modes of set *B*. For each principal strain axis, *e.g.* $[111]_I$, the different shear systems of set *A* give crystallographically equivalent solutions, as do those of set *B*.

3. Method of analysis

The analyses are based on the matrix algebra method of Wechsler, Liebermann & Read (1953) as restated by Weschsler (1959) for the generalized lattice-invariant shear, and on the graphical method of Liebermann (1958). In the graphical method the Wulff nets used had a radius of 15 cm. The mathematical method was modified to include an additional similarity transformation from an orthonormal basis [*e.g.* basis vectors $\left(\frac{1}{\sqrt{2}}\ -\frac{1}{2}\ 0\right)$, $\left(\frac{1}{\sqrt{6}}\ \frac{1}{\sqrt{6}}\ -\frac{2}{\sqrt{6}}\right)$, $\left(\frac{1}{\sqrt{3}}\ \frac{1}{\sqrt{3}}\ \frac{1}{\sqrt{3}}\right)$]

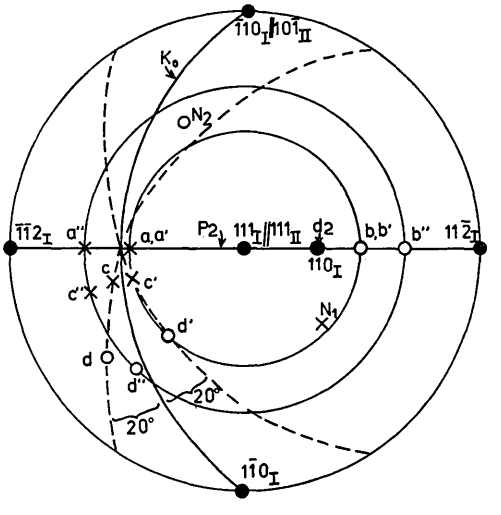

Fig. 3. Transformation geometry based on the lattice-invariant shear $(1\bar{1}0)\,[110]_I$. The stereogram shows initial (inner) and final (outer) cones of unextended vectors and some of the essential features of the graphical analysis. The contraction (strain) axis is $[111]_I$. For a shear angle $\sim -20°$, vectors **a** and **c** in the parent (NaCl) phase undergo both the L.I. shear and the lattice deformation without change in magnitude or included angle. The analysis is completed by the rigid-body rotation which returns these vectors to their initial positions *i.e.* $\mathbf{a}^{11}, \mathbf{c}^{11} \rightarrow \mathbf{a}, \mathbf{c}$. The habit plane ($N_1$) is the plane which contains **a** and **c**. Vectors **b** and **d** are another such pair of vectors (habit plane N_2). The other pairs of vectors are related to **a**, **c** and **b**, **d** by reflexion in $(1\bar{1}0)_I$. These require a L.I. shear $\sim 20°$. The corresponding solutions are crystallographically equivalent to those based on **a**, **c** and **b**, **d**. See Tables 2 and 4. $P2$ = L.I. shear plane, $d2$ = L.I. shear direction, K_0 = plane perpendicular to $d2$ and $P2$.

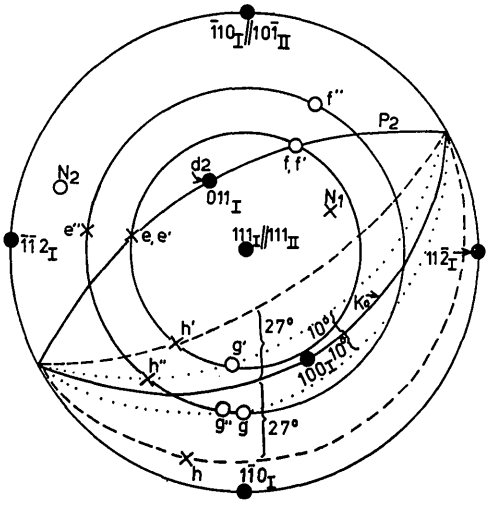

Fig. 4. Transformation geometry based on the lattice-invariant shear $(001)\,[011]_I$. This stereogram shows the initial (inner) and final (outer) cones of unextended vectors and some of the essential features of the graphical analysis. The contraction (strain) axis is $[111]_I$. For a shear angle $\sim 10°$, vectors **e** and **g** undergo both the L.I. shear and the lattice deformation without change in magnitude or included angle. The analysis is completed by the rigid-body rotation which returns these vectors to their initial positions, *i.e.* $\mathbf{e}^{11}, \mathbf{g}^{11} \rightarrow \mathbf{e}, \mathbf{g}$. The habit plane ($N_1$) is the plane which contains **e** and **g**. For a L.I. shear $\sim 27°$ vectors **f** and **h** are another such pair of vectors (habit plane N_2). One other pair of vectors exists for each of the L.I. shears and can be located by reflexion in $(0\bar{1}1)_I$. All four solutions lead to crystallographically equivalent results (Tables 3 and 5). $P2$ = L.I. shear plane, $d2$ = L.I. shear direction, K_0 = plane perpendicular to $P2$ and $d2$.

in which the lattice deformation matrix has the simple form

$$\begin{pmatrix} \eta & 0 & 0 \\ 0 & \eta_2 & 0 \\ 0 & 0 & \eta_3 \end{pmatrix},$$

to the usual cubic basis consisting of unit vectors in the $[100]_I$, $[010]_I$ and $[001]_I$ directions. The entire algorithm was then programmed in FORTRAN IV for use on a CDC 6400 computer. All tabulated predictions in this paper were obtained by means of this program.

4. Results

4.1 *Multiplicity of solutions*

Each of the six $\{110\}\ \langle 001\rangle_{II}$ slip systems can be combined with each $\langle 111\rangle$ strain axis. As there are four solutions for each combination there are 24 solutions per axis. For the four strain axes there are 96 solutions. The mathematical solutions however are of three different types. Within each type there are 24 distinct variants. These are equivalent by symmetry but physically distinguishable when any combination of them occurs. Two of the three types are produced by the lattice-invariant shear systems of Set *A*. They are marked (*a*) and (*b*) respectively in Tables 2 and 4. The

third type arises from the lattice-invariant shears of Set *B*. These when treated as slip, lead to 48 crystallographically equivalent possibilities (Tables 3 and 5). However, solutions which arise from the same lattice-invariant shear combined with different strain axes, which are mirror-related in the lattice-invariant shear plane (*e.g.* $[111]_I$, $[\bar{1}11]_I$ combined with $(100)\,[011]_I$), have the same habit plane and shape change, and have orientations which are related by $\{110\}_{II}$ mirror planes and are therefore also indistinguishable. The number of physically distinguishable solutions is thus reduced to 24. If the lattice-invariant shear occurs by twinning, the number of distinguishable variants is also 24, the resulting lattice being untwinned. If all three types of solution occurred, the maximum number of observable variants would be 72.

4.2 *Values*

Table 1 shows the magnitude of the strains in the lattice deformation. The lattice parameters are from Pöyhönen (1960) (NH_4Cl), Pöyhönen, Mansikka & Heiskanen (1964) (NH_4Br), Hovi & Varteva (1965) and Pöyhönen & Ruuskanen (1964) (CsCl). The orientation relations are shown in Tables 2 and 3 by stating in column 5 how far the product is rotated, around the axis shown in column 4, from the orientation $[111]_I \| [111]_{II}$, $(\bar{1}10)_I \| (\bar{1}01)_{II}$. Throughout the tables the contraction axis of the pure strain is indexed as [111]. Directions are stated as indices with fractional values. For convenience in initial experimental observations the approximate orientations of the habit planes may be noticed. They are 5° from $\{310\}_I$, 10° from $\{\bar{1}11\}$ (Table 2) and 5° from $\{210\}_I$ (Table 3). Tables 4 and 5 which show the effect of a $\pm 2\%$ uniform dilatation in the interface in either phase, would also apply to substances in which the ratio of the lattice parameters differs within 2% from the values in Tables 2 and 3. Transformation geometries are illustrated in Figs. 3 and 4, and orientation relations in Figs. 5, 6 and 7.

5. Discussion

Noteworthy features of the predictions are the large shape changes, the large number of variants, and the large differences between the orientation relations and the relation corresponding to the pure strain alone.

As an example of predicted shape change, solutions 1(*a*) and 2(*a*) of Table 2 imply that an initially cubic volume of crystal would change its interedge angles from 90 to 95, 118 and 117° approximately. Edge lengths would change by −15, +34 and +3%. The shape changes of Table 3 are less severe, but still large: interedge angles change from 90 to 79, 79 and 109° whilst edge lengths change by −11, +3 and +3%. As the three different types of solution imply different displacements, it may be anticipated that only one type would correspond to the physical mechanism under particular conditions. Up to 24 variants would then be obtained.

For a given lattice deformation and lattice-invariant shear, the predictions depend only upon the ratio $a_I : a_{II}$. Because this ratio is very similar for all the substances treated in this work, orientations and shape strains are also very similar. The main effect of a 2%

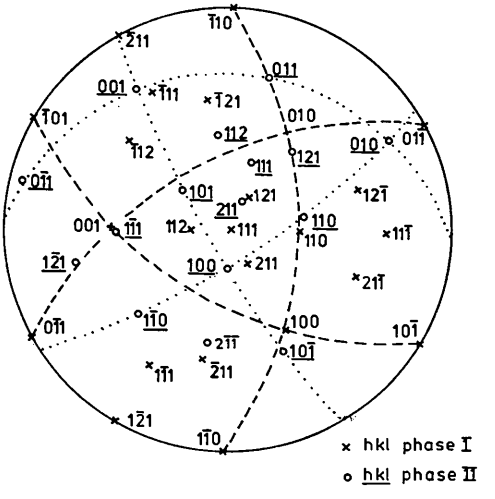

Fig. 5. Orientation relations: type 1. This O.R. is associated with solution 1(*a*)–NH_4Br of Table 2. Angles between rational poles or directions are listed here. Bracketed values refer to the corresponding solutions 1(*a*) of Table 4, with $a_I/a_{II} = 1{\cdot}645$ and 1·711 respectively: $(001)_I \wedge (1\bar{1}1)_{II} = 2{\cdot}24°$ (3·77°, 0·83°), $(100)_I \wedge (10\bar{1})_{II} = 9{\cdot}02°$ (5·93°, 12·7°), $(110)_I \wedge (11\bar{0})_{II} = 6{\cdot}40°$ (10·68°, 2·70°), $[111]_I \wedge [11\bar{1}]_{II} = 35{\cdot}25°$ (38·04°, 32·49°). Solution 1(*a*)–CsCl of Table 2 predicts the following angles: $(001)_I \wedge (1\bar{1}1)_{II} = 2{\cdot}35°$, $(100)_I \wedge (10\bar{1})_{II} = 8{\cdot}75°$, $(110)_I \wedge (110)_{II} = 6{\cdot}55°$, $[111]_I \wedge [11\bar{1}]_{II} = 35{\cdot}46°$.

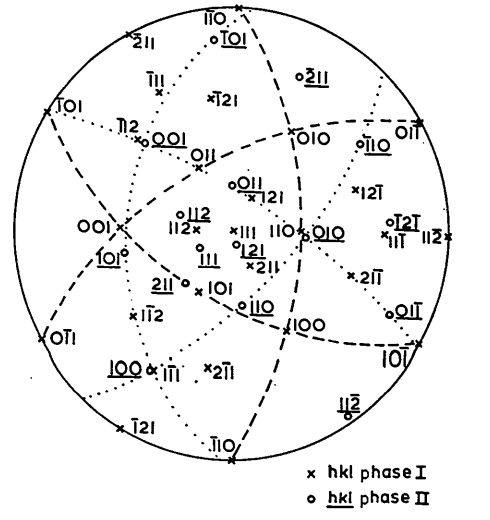

Fig. 6. Orientation relations: type 2. This O.R. is associated with solution 1(*b*)–NH_4Br of Table 2. Bracketed values of angles apply to the corresponding solutions 1(*b*) of Table 4 with $a_I/a_{II} = 1{\cdot}645$ and 1·711 respectively: $(110)_I \wedge (010)_{II} = 3{\cdot}55°$ (2·90°, 4·30°), $(1\bar{1}1)_I \wedge (100)_{II} = 0{\cdot}32°$ (0·42°, 0·10°), $[111]_I \wedge [11\bar{1}]_{II} = 19{\cdot}06°$ (19·44°, 18·56°). Solution 1(*b*)–CsCl of Table 2 predicts the following angles: $(110)_I \wedge (010)_{II} = 3{\cdot}45°$, $(1\bar{1}1)_I \wedge (100)_{II} = 0{\cdot}45°$, $[111]_I \wedge [11\bar{1}]_{II} = 19{\cdot}09°$.

relative dilation of one phase is to rotate one of the sets of orientation relations by 4°.

The calculations should similarly apply to transformations at both normal and high pressures. Whilst values of lattice parameters at the transformation pressure P_{tr} are available only for one phase, available data suggest that the ratio $a_I:a_{II}$ is close to that at atmospheric pressure. For example with the lattice parameters given by Evdokimova & Vereshchagin (1962) the ratios a_I(atmospheric pressure)/a_{II}(transformation pressure) for RbCl and RbI respectively are $1{\cdot}71_7$ and $1{\cdot}68_7$. Since a_I will be smaller at higher pressure, the ratios will tend towards the lower value in the Tables, 1·675.

No explicit allowance for the presence of charged ions in the structure seems necessary, for these centrosymmetric structures do not introduce problems of electrically polarized domains as in the ferroelectrics, and the twinning systems used do not introduce the relatively high-energy {111} stacking faults.

The experimental data available for comparison are mainly orientation relations. However, Livshitz *et al.* (1969) reported lamellar, possibly martensitic, morphology produced in the pressure-induced transformations NaCl → CsCl → NaCl-type in KCl; and Fraser & Kennedy (1972) observed regular shape changes induced by the transformation NaCl-type → CsCl-type in plate-like crystals of NH_4Br measuring $50\times50\times5$ μm. The interedge angles of some fully transformed regions became 80 and $82\pm3°$ in different specimens. Current work reveals oriented platelets. The several orientations of traces already measured are consistent with the predicted habit planes. In orientation data, allowance must be made for lack of precision due to plastic deformation in X-ray specimens, and to the difficulty of fixing precise orientation in electron diffraction. An orientation approximating to the type $\{100\}_I\|\{110\}_{II}$, $\langle010\rangle_I\|\langle\bar{1}11\rangle_{II}$ was reported by Fraser & Kennedy (1972) for NH_4Br, and suggested as possible by Pöyhönen, Jaakkola & Räsänen (1964) and Chatterji, Mackay & Jeffery (1970) for CsCl. The sets of solutions 1(*a*) and 2(*a*) of Tables 2 and 4 can account for this relation. Lüdemann (1957), studying epitaxically grown films of CsCl by electron diffraction, found that they transformed from the NaCl structure maintaining $(001)_I\|(111)_{II}$, $[\bar{1}10]_I$ or $[110]_I\|[11\bar{2}]_{II}$. This is very close to the type of relation predicted in Table 3. The calculations therefore predict most observed orientations within experimental error. There is, however, another relation, which approximates to $\{100\}_I\|\{100\}_{II}$, $\langle010\rangle_I\|\langle101\rangle_{II}$ observed by Fraser & Kennedy (1972) and again suggested as a possibility by Pöyhönen *et al.* (1964) and Chatterji *et al.* (1970). Kennedy, Patterson, Chaplin & Mackay (1974) have observed this type of relation in the reverse transformation and have suggested how it might arise as a secondary orientation through stacking of twins due to symmetry options, but no very close approximation due to stacking of variants is apparent from the present work. An explanation of this remaining relation might be sought either in another lattice-invariant shear system, or in another mechanism probably involving an alternative lattice correspondence.

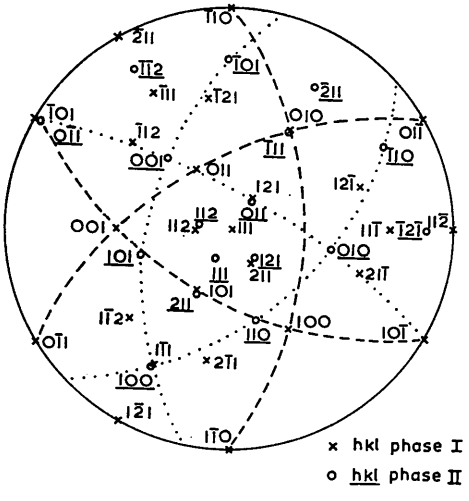

Fig. 7. Orientation relations: type 3. This O.R. is associated with solution 2(*a*)–NH_4Br of Table 3. The two bracketed values of angles in the following list apply to the corresponding solution 2(*a*) of Table 5 with $a_I/a_{II}=1{\cdot}645$ and 1·711 respectively: $(101)_I\wedge(211)_{II}=1{\cdot}68°$ (2·67°, 0·65°), $(010)_I\wedge(\bar{1}11)_{II}=1{\cdot}27°$ (1·92°, 0·53°), $[111]_I\wedge[111]_{II}=16{\cdot}95°$ (16·27°, 17·52°). Solution 2(*a*)–CsCl of Table 3 predicts the following angles: $(101)_I\wedge(211)_{II}=1{\cdot}95°$, $(010)_I\wedge(\bar{1}11)_{II}=1{\cdot}58°$, $[111]_I\wedge[111]_{II}=17{\cdot}00°$.

In experiments, the product might sometimes appear polycrystalline if a large number of the variants occur within a parent crystal. Additional nucleation centres might be activated by stresses due to the variant formed first. This large number of possible variants would account for the difficulty found in earlier experimental studies in defining specific relations, and for the reports of polycrystalline products (Menary, Ubbelohde & Woodward, 1951).

The large shape change might autocatalyse formation of specific further variants which, in combination with the first, would reduce the resulting strains and stresses. Stacking of sets of variants which have different shape strains could reduce the total shape change of the specimen. In contrast, random juxtaposition of variants would cause stresses which could cause plastic deformation subsequent to the transformation, and possible fracture.

The work was supported by the Australian Research Grants Committee.

References

Bowles, J. S. & Mackenzie, J. K. (1954). *Acta Met.* **2**, 129–147.

Bowles, J. S. & Wayman, C. M. (1972). *Metall. Trans.* **3**, 1113–1121.

BUERGER, M. J. (1951). In *Phase Transformations in Solids*. Edited by R. SMOLUCHOWSKI, J. E. MAYER & W. A. WEYL. New York: John Wiley.
BUERGER, M. J. (1961). *Fortschr. Mineral.* **39**, 9–23.
CHATTERJI, S., MACKAY, A. L. & JEFFERY, J. W. (1971). *J. Appl. Cryst.* **4**, 175.
CHRISTIAN, J. W. (1965). *The Theory of Transformations in Metals and Alloys*. Oxford: Pergamon.
EVDOKIMOVA, V. V. & VERESHCHAGIN, L. F. (1962). *Sov. Phys. JETP*, **43**, 1208–1212.
FRASER, W. L. & KENNEDY, S. W. (1972). *Acta Cryst.* B**28**, 3101.
HOVI, V. & VARTEVA, M. (1965). *Phys. Kondens. Mater.* **3**, 305–310.
KELLY, A. & GROVES, G. W. (1970). *Crystallography and Crystal Defects*. London: Longmans.
KENNEDY, S. W., PATTERSON, J. H., CHAPLIN, R. P. & MACKAY, A. L. (1974). *J. Solid State Chem.* **9** (No. 4). In the press.
LIEBERMAN, D. S. (1958). *Acta Met.* **6**, 680–693.
LIVSHITZ, L. D., RYABININ, Y. N., LARIONOV, L. V. & ZVEREV, A. S. (1969). *Sov. Phys. JETP*, **28**, 612–613.
LÜDEMANN, H. (1957). *Z. Naturforsch.* **12a**, 226–228.
MENARY, J. W., UBBELOHDE, A. R. & WOODWARD, I. (1951). *Proc. Roy. Soc.* A**208**, 158–169.
OWEN, W. S. & SCHOEN, F. J. (1971). *Structural Characteristics of Materials*, Chap. 4. Edited by H. M. FINNISTON. London: Elsevier.
PÖYHÖNEN, J. (1960). *Ann. Acad. Sci. Fenn.* **AVI**, No. 58.
PÖYHÖNEN, J., JAAKKOLA, S. & RÄSÄNEN, V. (1964). *Ann. Univ. Turku. A*, No. 80.
PÖYHÖNEN, J., MANSIKKA, K. & HEISKANEN, K. (1964). *Ann. Acad. Sci. Fenn.* **AVI**, No. 168.
PÖYHÖNEN, J. & RUUSKANEN, A. (1964). *Ann. Acad. Sci. Fenn.* **AVI**, No. 146.
RACHINGER, W. A. & COTTRELL, A. H. (1956). *Acta Met.* **4**, 109–113.
SHOJI, H. (1931). *Z. Kristallogr.* **77**, 381–397.
WAYMAN, C. M. (1964). *Introduction to the Crystallography of Martensitic Transformations*. New York: Macmillan.
WECHSLER, M. S. (1959). *Acta Met.* **7**, 793–802.
WECHSLER, M. S., LIEBERMAN, D. S. & READ, T. A. (1953). *Trans. AIME*, **197**, 1503–1515.
ZINTL, E. & BRAUER, G. (1935). *Z. Electrochem.* **41**, 102–107.

Acta Cryst. (1974). A**30**, 22

Structural Studies by High-Resolution Electron Microscopy: Tetragonal Tungsten Bronze-Type Structures in the System Nb_2O_5–WO_3

BY S. IIJIMA*
Department of Physics, Arizona State University, Tempe, Arizona 85281, *U.S.A.*
AND J. G. ALLPRESS
Division of Tribophysics, CSIRO, University of Melbourne, Parkville, Victoria, 3052, *Australia*

(*Received* 14 *March* 1973; *accepted* 12 *April* 1973)

The contrast in many-beam lattice images from very thin crystals of $4Nb_2O_5.9WO_3$ is shown to be directly related to its known structure. On the basis of this correlation, the structure of $2Nb_2O_5.7WO_3$ is derived from the observed image contrast; it is an ordered intergrowth of the ReO_3 and tetragonal tungsten bronze structural types. The structures of typical fault boundaries and disordered intergrowths are described, and those of the reported compounds $6Nb_2O_5.11WO_3$ and $3Nb_2O_5.8WO_3$ are discussed.

1. Introduction

The binary system Nb_2O_5–WO_3 has been the subject of a great deal of structural investigation during recent years, and at least ten distinct phases have been recognized by X-ray methods (Roth & Waring, 1966). The dominant structural unit in all these phases is the MO_6 octahedron, which, in general, shares its corner oxygen atoms with neighbours to build up a three-dimensional lattice. In one crystallographic direction through the structures, the octahedra always form linear strings, with a simple repeat distance of about 0·38 nm, corresponding to the length of a body diagonal. Differences between the structures arise from variations in the arrangement of octahedra in the remaining two directions, and two major structural types can be distinguished:

(*a*) Crystallographic shear (CS) structures, in which the octahedra are joined as in ReO_3 [Fig. 1(*a*)], into blocks or slabs, and neighbouring slabs are joined by sharing octahedral edges rather than corners. This description applies to the Magnéli phases (>90 mole % WO_3), and to the Nb_2O_5-type of block structures (<48 mole % WO_3).

(*b*) Tunnel structures, in which the octahedra are joined in a more complex way, leaving tunnels of various shapes, some of which may be filled by additional ions. These include WNb_2O_8, and several structures containing 64–78 mole % WO_3, which share a common

* On leave from the Research Institute for Scientific Measurements, Tohoku University, Sendai, Japan.